whereas the curve profiles tend to retain the characteristics of regime I over more of their length as the molecular weight increases.

We see then that the presence of cilia nucleation as suggested by Sanchez and DiMarzio is compatible with the regime theory of Hoffman and Lauritzen, for the existence of regimes may be due to the density of cilia per unit length of growth strip being dependent on the molecular weight. The rate at which the character of the growth changes from regime I to regime II, and the undercooling at which this occurs, appears to vary with molecular weight. However, a test of this hypothesis for dilute solution crystallization will require extension of the growth rate measurements to higher and lower undercoolings using well fractionated polymer samples. Unfortunately, using present techniques, meaningful growth rate measurements of polyethylene crystallization cannot be made outside of the range reported here. The higher molecular weight fractions could be studied at slightly smaller undercoolings, but any extension of the range of study for the remaining samples would lead to a marked loss in precision because of the very slow or very rapid growth rates involved, rendering the results of but little value.

References and Notes

(1) J. I. Lauritzen, Jr., and J. D. Hoffman, *J. Res. Nat. Bur. Stand., Sect. A*, **64**, 73 (1960).
(2) F. C. Frank and M. Tosi, *Proc. Roy. Soc., Ser. A*, **263**, 323 (1961).
(3) F. P. Price, *J. Chem. Phys.*, **35**, 1884 (1961).
(4) J. D. Hoffman, *SPE, (Soc. Plast. Eng.) Trans.*, **4**, 315 (1964).
(5) J. I. Lauritzen, Jr., and E. Passaglia, *J. Res. Nat. Bur. Stand., Sect. A*, **71**, 261 (1967).
(6) I. C. Sanchez and E. A. DiMarzio, *J. Chem. Phys.*, **55**, 893 (1971).
(7) I. C. Sanchez and E. A. DiMarzio, *Macromolecules*, **4**, 677 (1971).
(8) L. H. Tung, J. C. Moore, and G. W. Knight, *J. Appl. Polym. Sci.*, **10**, 1261 (1966).
(9) A. Peyrouset and R. Panaris, *J. Appl. Polym. Sci.*, **16**, 315 (1972).
(10) D. J. Blundell, A. Keller, and A. J. Kovacs, *J. Polym. Sci., Part B*, **4**, 481 (1966).
(11) D. J. Blundell and A. Keller, *J. Macromol. Sci., Phys.*, **2**, 301 (1968).
(12) D. J. Blundell and A. Keller, *J. Polym. Sci., Part B*, **6**, 443 (1968).
(13) T. Seto, and N. Mori, *Rep. Progr. Polym. Phys. Jap.*, **12**, 157 (1969).
(14) A. Keller and E. Pedemonte, *J. Cryst. Growth*, **18**, 11 (1973).
(15) I. C. Sanchez and E. A. DiMarzio, *J. Res. Nat. Bur. Stand., Sect. A*, **76**, 213 (1972).
(16) V. F. Holland and P. H. Lindenmeyer, *J. Polym. Sci.*, **57**, 589 (1962).
(17) M. Cooper and R. St. J. Manley, *J. Polym. Sci., Polym. Lett. Ed.*, **11**, 363 (1973).
(18) D. Turnbull and R. L. Cormia, *J. Chem. Phys.*, **34**, 820 (1961).
(19) J. J. Weeks, unpublished data as communicated to Sanchez and DiMarzio.
(20) T. W. Huseby and H. E. Bair, *J. Appl. Phys.*, **39**, 4969 (1968).
(21) J. F. Jackson and L. Mandelkern, *Macromolecules*, **1**, 546 (1968).
(22) A. Nagajima, S. Hayashi, T. Korenaga, and T. Sumida, *Kolloid-Z. Z. Polym.*, **222**, 124 (1968).
(23) T. Korenaga, F. Hamada, and A. Nakajima, *Polym. J.*, **3**, 21 (1972).
(24) E. Ergoz and L. Mandelkern, *J. Polym. Sci., Polym. Lett. Ed.*, **11**, 73 (1973).
(25) L. Mandelkern, J. G. Fatou, and C. Howard, *J. Phys. Chem.*, **68**, 3386 (1964).
(26) T. Kawai, *J. Polym. Sci., Part B*, **2**, 965 (1964).
(27) J. D. Hoffman, J. I. Lauritzen, Jr., G. S. Ross, and L. Frolen, to be published.
(28) J. D. Hoffman, G. T. Davis, and J. I. Lauritzen, Jr., "Treatise on Solid State Chemistry," Hannay, Ed., to be published.
(29) J. D. Hoffman and J. I. Lauritzen, Jr., *J. Appl. Phys.*, **44**, 4340 (1973).
(30) J. D. Hoffman, personal communication.
(31) P. J. Flory and A. Vrij, *J. Amer. Chem. Soc.*, **85**, 3548 (1963).
(32) A. J. Pennings, "Characterization of Macromolecular Structure," publication No. 1573 of the National Academy of Science, Washington, D.C., 1968, p 214.
(33) J. D. Hoffman, J. I. Lauritzen, Jr., E. Passaglia, G. S. Ross, L. J. Frolen, and J. J. Weeks, *Kolloid-Z. Z. Polym.*, **231**, 564 (1969).
(34) A. M. Rijke and L. Mandelkern, *J. Polym. Sci., Part A-2*, **8**, 225 (1970).
(35) J. I. Lauritzen, Jr., *J. Appl. Phys.*, **44**, 4353 (1973).

Thermally Induced Phase Separation Behavior of Compatible Polymer Mixtures

T. Nishi,[1] T. T. Wang, and T. K. Kwei*

Bell Laboratories, Murray Hill, New Jersey 07974. *Received October 31, 1974*

ABSTRACT: Thermally induced phase separation behavior of polystyrene–poly(vinyl methyl ether) mixtures has been studied by light transmission, optical microscope, and pulsed nmr methods. It is found that the polymer pair can phase separate by spinodal mechanism or by nucleation and growth depending upon composition and temperature. Direct proof of spinodal decomposition is provided by the nmr data which indicate a gradual change in the composition of the new phases but little change in the volumes of precipitating phases during decomposition. In addition, using the nmr data it is possible to estimate the parameters governing the kinetics of spinodal decomposition. The coefficient of diffusion is found to be negative, indicating that phase separation has taken place by the characteristic uphill diffusion. Large differences in light transmission and morphological behavior are noted during the early stages of decomposition under the two mechanisms. Most noteworthy are residual turbidity found in the sample which has apparently undergone spinodal decomposition, the high degree of interconnectivity in the spinodal structure, and the rapid rate with which such a structure is formed. The residual turbidity reaches a maximum in the PS–PVME = 20:80 mixture. By contrast, samples which have undergone phase separation by nucleation and growth exhibit no residual turbidity; the precipitating phase domains are discrete and the formation of the phase pattern is relatively slow.

In previous publications,[2] the compatibility and phase separation behavior of solvent cast polystyrene (PS)–poly(vinyl methyl ether) (PVME) films were investigated over a wide range of compositions and temperatures. The study revealed among other things the existence of a cloud point curve associated with a lower critical solution temperature.[2b,3] The result strongly suggests that there may be an unstable region within the miscibility gap where phase separation could take place by spinodal mechanism rather than by nucleation and growth.[4,5] Although the spinodal decomposition behavior has been investigated for a few polymer–solvent[6,7] and polymer–polymer[8] systems, knowledge of such phenomenon is still rather limited, especially in regard to the basic parameters which govern the spinodal decomposition process.

Earlier[2a] it has been demonstrated that the volume fractions as well as the composition of phases in the PS–PVME system can be determined with relative ease by the pulsed nmr technique. Since one of the important characteristics which differentiates the spinodal mechanism from nuclea-

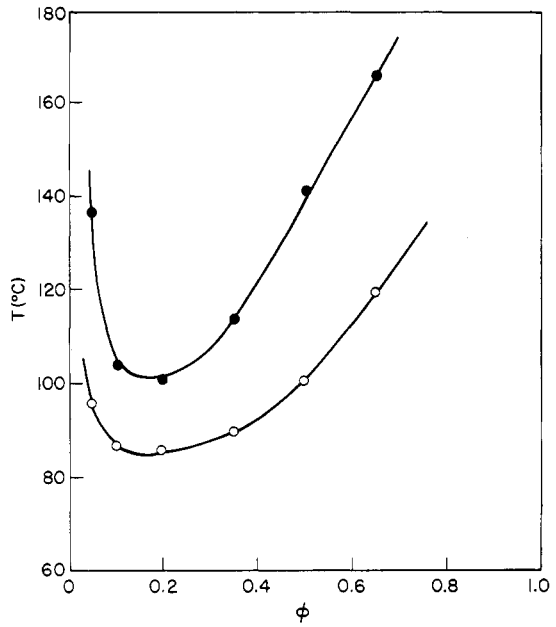

Figure 1. Plot of the initiation temperatures (○) and apparent completion temperatures (●) of phase separation for several PS concentrations, ϕ, of PS–PVME mixtures. The heating rate is 0.2°C/min.

tion and growth is the continuous change of composition of phases during phase separation,[4] the nmr technique should be quite suitable for determining not only the mechanism by which the phase separates but also, in the case of spinodal decomposition, the basic parameters governing such a process. In this paper we report the thermally induced phase separation behavior of PS–PVME mixtures as examined by nmr, light transmission, and optical microscope methods, and attempt to determine the parameters characterizing the kinetics of spinodal decomposition.

Experimental Section

Materials. A monodisperse PS with a nominal molecular weight of 200,000 was obtained from the Pressure Chemical Co. The ratio between the weight average and number average molecular weights, $\bar{M}_w/\bar{M}_n$, was 1.06. PVME, supplied by Cellomer Associates, Inc., was purified by precipitating twice from benzene solution to an excess volume of methanol. The weight average molecular weight of the purified material, as determined from an intrinsic viscosity of 0.51 in benzene, was 51,500. Films of PS and PVME mixtures were cast from toluene solution as described in a previous publication.[2a]

1. Measurements of Thermochromatic Properties. A sample about 5 mm square was cut from the cast film and mounted on a 1 mm thick slide glass. Thin (0.2 mm) airtight spacers were placed around the specimen and a 0.16 mm thick cover glass was applied to protect the sample. The assembly was heated above the glass transition temperature, T_g, of the polymer mixture, then carefully pressed down to form a uniformly thick sample free of air space between the glasses and the sample. The assembly was slowly cooled down to relieve any stresses induced in the operation. To measure the light transmission the sample assembly and the hot stage were mounted on the microscope, and the sample was illuminated with polarized light. With the optical analyzer set parallel to the polarizer the intensity of transmitted light was monitored with a photocell at the eyepiece position and recorded as an output voltage on a recorder. During the experiment the sample temperature was regulated with a Mettler FP5 control unit and an FP52 hot stage. Calibration of hot stage temperature was accomplished by means of the triple points of naphthalene (80.24 ± 0.05°) and adipic acid (151.46 ± 0.05°) using the present sample geometry.

2. Microscopic Observation. A thin film of PS and PVME mixture was cast from toluene solution onto the slide glass and dried under vacuum above its T_g for at least 24 hr. A cover glass was placed on top of the film and, upon heating to above T_g of the polymer mixture, the assembly was gently pressed to form a 5-μm thick film between the glasses, then allowed to cool slowly to room temperature. To observe the phase separation behavior the assembly was placed in a hot stage mounted on the microscope and heated at the rate of 10°C/min to about 5° below the phase separation temperature of the polymer mixture. After holding at this temperature for at least 5 min to ensure even temperature distribution in the sample, the assembly was quickly brought up to the desired temperature and maintained there while the phase change was observed with a phase contrast lens. In some cases, samples were quenched from the test temperature to −45° with an organic liquid before they were examined with a high magnification lens at room temperature.

3. Nmr Measurements. Details of pulsed nmr apparatus and measurement procedure have been described elsewhere.[2a,9] The isothermal phase transformation treatment of the sample was made in a silicone oil bath controlled to within ±0.1°. Prior to the heat treatment the sample was vacuum sealed in a thin walled (~0.5 mm) nmr tube and warmed up in the air immediately above the oil bath to about 10° below the phase separation temperature of the sample. After about 3 min at this temperature, the sealed sample was quickly immersed in the oil bath for a desired length of time, followed by rapid quenching in liquid nitrogen. While the sample was still at liquid nitrogen temperature, it's spin–lattice relaxation time T_1 was measured by applying a 180°–τ–90° pulse sequence. For thermal treatment of very short duration (20 sec), samples were sandwiched between thin aluminum foils and immersed in the oil bath. They were packed and vacuum sealed in an nmr tube after quenching. In some cases, measurements were made above room temperature up to 60° and the results did not change appreciably during the test period. The data were analyzed according to the procedure already described in a previous publication.[2a] In calculating PVME per cent in the PS-rich phase in the phase separated samples, the spin diffusion effect[10,11] in each phase and no coupling between the phases[12] were assumed, which seems to be valid in this system.[2a]

Results

1. Thermochromatic Properties. Figure 1 shows the composition dependence of the phase separation behavior as the sample temperature was being raised. Reproducibility of the data was found to be within the bounds of experimental error. The lower and upper curves indicate respectively the initiation and completion of phase separation as measured by the light transmission instruments; initiation marks the temperature at which the transmitted light begins to decrease in its intensity while completion denotes the temperature when the light intensity levels off to a minimum. The lowest phase separation temperature, T_{min}, is found at around $\phi \simeq 0.2$, where ϕ is the volume fraction of PS (hereafter this composition will be referred to as ϕ_{min}). Concurrently the temperature gap between the initiation and the completion appears to also be at its minimum at ϕ_{min}. It was found, however, that the thermochromatic property of the sample differed markedly depending on whether its composition was near ϕ_{min} or far removed from ϕ_{min}. Typical examples are shown in Figures 2 and 3 for 65:35 (PS–PVME) and 20:80 mixtures. For the 65:35 sample (Figure 2) the transmitted light intensity, I, starts to decrease at 120° on heating and keeps on decreasing gradually until it levels off at about 166°. Upon cooling, I exhibits its normal hysteresis behavior by tracing the lower curve until the film becomes transparent again.

For the 20:80 sample (Figure 3), on the other hand, I shows a rapid change on heating but a gradual and steady change on cooling, thereby causing the two curves to cross one another. Moreover, during the cooling process the film does not regain its transparency completely until it reaches a lower temperature. This apparent irreversibility in phase separation behavior can be studied in terms of residual turbidity, τ_R, defined as

$$\tau_R = (1/d) \ln (I_0/I_R) \quad (1)$$

where d is the sample thickness and I_0 and I_R are respec-

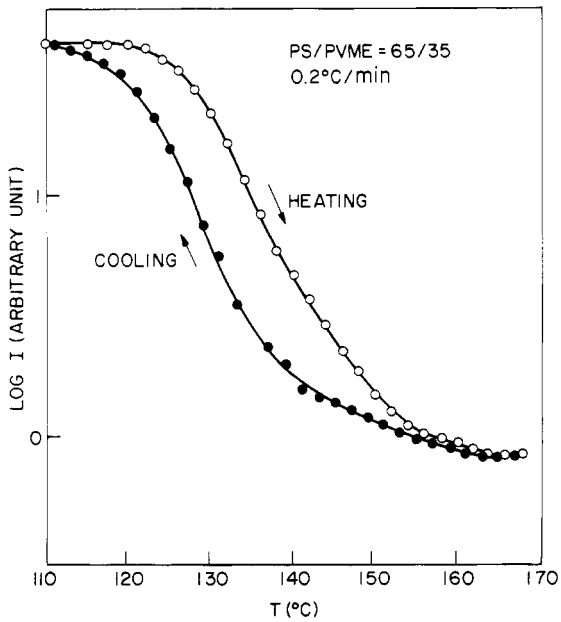

Figure 2. Thermochromatic properties of the PS–PVME = 65:35 mixture.

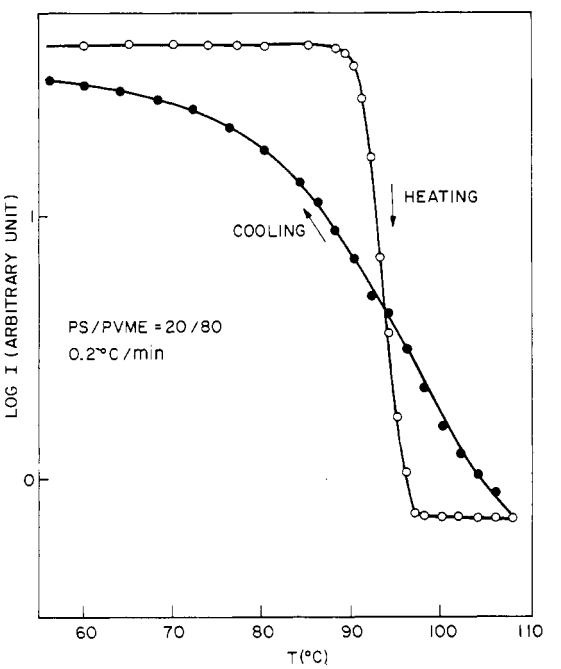

Figure 3. Thermochromatic properties of the PS–PVME = 20:80 mixture.

the variation of I with time. Typical results for samples light intensity after cooling. Figure 4 displays the residual turbidity, τ_R, as a function of the volume fraction, ϕ, of PS at several heating rates. Several features appear to be worth noting, namely, all curves have a maximum at around ϕ_{min} and the peak of the curve becomes sharper as the rate of heating is increased. In addition, while these maximum τ_R's are much smaller than the maximum turbidities attained at the completion of phase separation (250 to 300 cm^{-1}), they are much larger than the so-called bluish coloration and white opalescence[2b,3,13] of the film which is about 1–2 cm^{-1} for the former and 20–30 cm^{-1} for the latter in our experiments.

These anomalies were further confirmed by repeatedly changing the temperature of the sample slightly below and above the phase separation temperature while monitoring

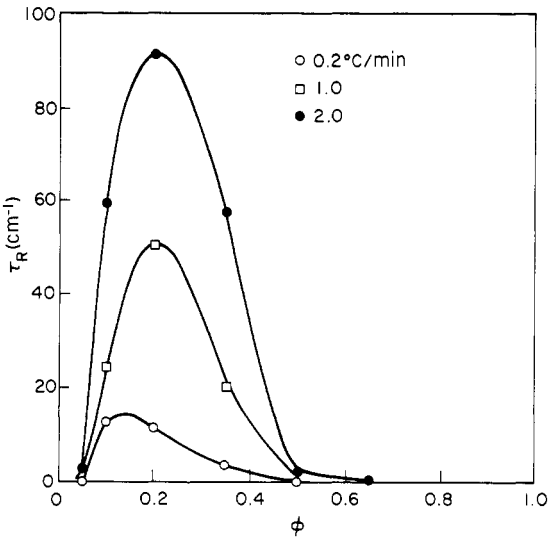

Figure 4. Variations of apparent residual turbidity τ_R with PS concentration, ϕ, and rate of temperature change for PS–PVME mixtures after cooling.

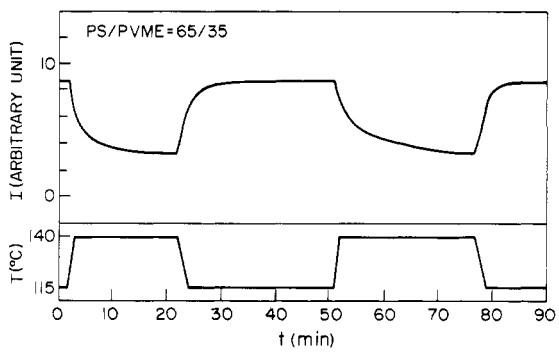

Figure 5. Plot of light intensity, I, *vs.* time, t, on repeated heating and cooling near the phase separation temperature of the PS–PVME = 65:35 mixture.

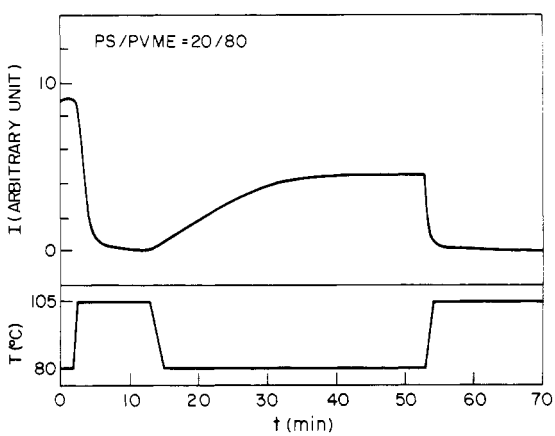

Figure 6. Plot of light intensity, I, *vs.* time, t, on repeated heating and cooling near the phase separation temperature of the PS–PVME = 20:80 mixture.

tively the initial light intensity before heating and residual 65:35 (PS–PVME) and 20:80 are shown in Figures 5 and 6, respectively. In Figure 5, with the sample temperature oscillating between 115 and 140° (lower figure) the time dependence of I is almost reproducible in each subsequent cycle and at the lower temperature the sample quickly recovers its transparency. On the other hand, the recovery is clearly slower and poorer for sample 20:80 as shown in Figure 6.

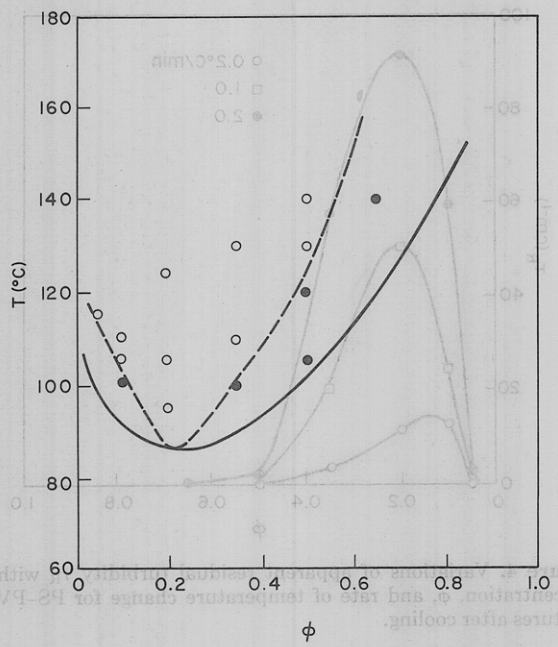

Figure 7. Several compositions (ϕ) and temperatures where phase separation by what appears to be spinodal mechanism (○) and nucleation and growth mechanism (●) are observed under a microscope. The dotted curve represents the line of demarcation of the two morphologies.

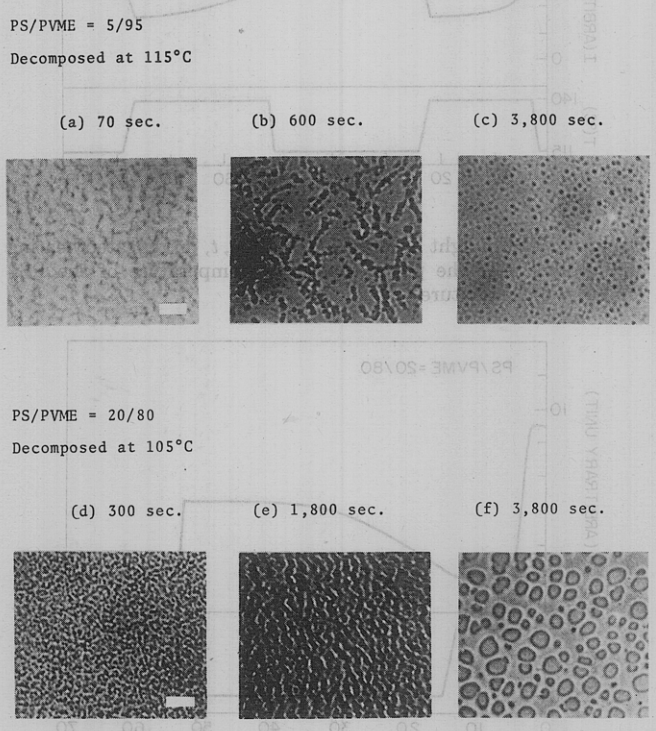

Figure 8. Time study of the phase separation behavior after the sample has been heated rapidly to and maintained at high temperatures (open circle condition in Figure 7). White bar in the figure corresponds to 10 μm. Phase patterns at different stages of decomposition are shown.

2. Microscopy. The circles in Figure 7 indicate the temperatures and compositions at which the polymer mixtures were examined under a phase contrast microscope. In general, the morphology which evolved during the phase separation looked rather uniform throughout the sample except near the edges where the thickness changed abruptly. On the basis of morphological observation, the phase separation behavior of the polymer mixtures may be divided into two categories whose features are as described below.

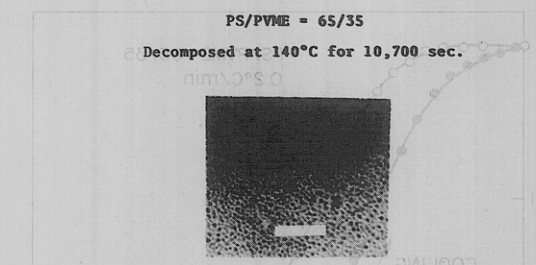

Figure 9. Phase separation by what appears to be nucleation and growth mechanism for the PS–PVME = 65:35 mixture. White bar in the figure corresponds to 10 μm.

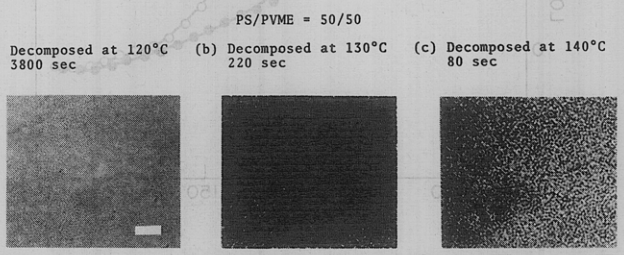

Figure 10. Initial phase separation pattern for PS–PVME = 50:50 decomposed at different temperatures. White bar in the figure corresponds to 10 μm.

Samples prepared according to conditions represented by open circles in Figure 7 follow. (i) The phase separation proceeded rapidly and the precipitated phases appeared to be interconnected with each other. (ii) Although the phase pattern did not show certain order, the dimension or spacing of the pattern was almost uniform. (iii) The phase pattern tended to be finer at higher decomposition temperature. (iv) At the later stage of phase separation the phase domains seemed to grow in size while maintaining their interconnectivity and developed into a reticular structure which eventually either broke up into small spheres or merged into macrospheres.

Samples prepared under conditions represented by filled circles in Figure 7 follow. (v) The phase separation proceeded rather slowly and the precipitated phase appeared in the form of spheres. (vi) These spheres were usually very small compared with the average spacings of phase patterns observed under conditions marked by open circles.

Several examples are given in Figures 8–10. The photomicrographs in Figure 8 show the time sequence morphologies of samples which had undergone isothermal phase transformation according to the open circle conditions. Figures 8a and 8d correspond to the initial stages of phase separation as described in (i) and (ii). After 10 to 30 min of aging, these patterns gradually give way to reticular structures, Figure 8b and Figure 8e, which finally break up into small spheres (Figure 8c) or merge into macrospheres (Figure 8f) as explained in (iv).

Figure 9 shows the phase separation behavior under the filled circle conditions, detail of which has been given in (v) and (vi).

If the composition was not far removed from ϕ_{min} one could observe both types of phase separation in the same sample as the annealing temperature was changed. An example is given in Figure 10 which displays the initial decomposition patterns of sample 50:50 aged at several temperatures. At 120° the phase transformation is suitably characterized by (v) and (vi) whereas at 130 and 140° the behavior changes to the other types depicted by (i) and (ii). In the latter cases (130 and 140°) the domain size decreases with temperature in accordance with (iii).

In addition to the morphological changes at various stages of phase separation the interconnectivity of phases at the initial stages of decomposition was examined by focusing the microscope at different points across the sample thickness. It was found that for samples obtained under open circle conditions, such as those shown in Figures 8d or 10b and 10c, the bright and dark domains tended to alternate their complexions in a slow and continuous manner as the focal point was varied, indicating a high degree of connectivity among domains of each phase. For samples prepared under filled circle conditions, such as those in Figures 9 or 10a, the color changes of the domains tended to be abrupt and discrete suggesting very little interconnectivity of the two phases.

3. Nmr Measurements. Figure 11 shows the spin–lattice relaxation times, T_1, of sample 50:50 prepared in the manner described earlier. The samples were isothermally annealed at 130° (which corresponds to open circle conditions in Figure 7) for periods ranging from 20 sec to 32 min, and the nmr data were measured at 50°. In the figure, the signal intensity S immediately following the 90° pulse is plotted against the pulse interval τ between 180 and 90° pulses. For the sake of clarity, all data from the same annealing time have been shifted along the τ axis by the same amount. The results clearly show two T_1's; the long T_1 becomes longer while the short T_1 becomes shorter as the annealing time is increased. Table I summarizes both the long and the short T_1's as well as the long T_1 component (in per cent) for each annealing time. As indicated in the table, the accuracy of two T_1's increases with decomposition time since the ratio of two T_1's increases with decomposition time from about 2.5 to 6. The confidence limits for extracting the two T_1's are almost in keeping with those reported in the literature.[14,15]

Since T_1's for pure PVME and PS are respectively 66 and 1400 msec at 50°,[2a] the shifting of the measured T_1's toward these two values clearly suggests a gradual change of PVME or PS concentration in each phase during the decomposition process. On the other hand, it will be noted that the long T_1 component remains nearly constant at 35% irrespective of the annealing time.

Discussion

From chromatic measurements of phase separation on heating, Figure 1, it is seen that the minimum temperatures for both initiation and completion occur at the PS concentration of about 0.2, *i.e.*, $\phi_{min} = 0.2$. This ϕ_{min} should coincide with the critical composition, ϕ_{crit}, although a slight difference may exist between the two because of the molecular weight distributions of the polymer components.[16,17] At ϕ_{crit} the spinodal and binodal curves converge but the temperature gap between them increases rapidly as the concentration deviates from ϕ_{crit}. In the region bounded by binodal and spinodal curves, where the phase is metastable, decomposition is known to be governed by nucleation and growth whereas within the spinodal, where the phase is unstable, precipitation is dictated by spinodal decomposition.[4,5]

The spinodal decomposition phenomenon has been studied in great detail by Cahn[4] and Hilliard.[5] According to Cahn, a partially miscible binary system can decompose spontaneously into two phases by uphill diffusion when it is suddenly brought from a single homogeneous phase into an unstable region. The uphill transport phenomenon can be described by including in the diffusion equation higher order terms which reflect the thermodynamic contributions of gradient energy terms. For the initial stages of decomposition, Cahn's formulation reduces to a linear equation

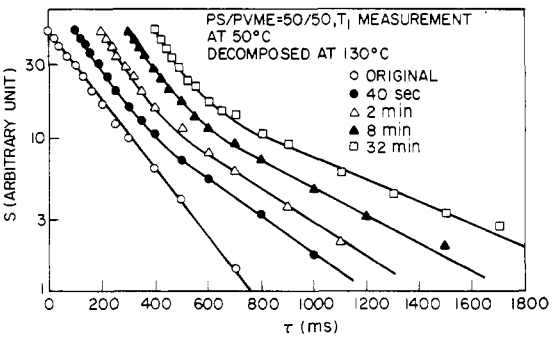

Figure 11. Spin–lattice relaxation measurements at 50° for PS–PVME = 50:50 decomposed at 130° for various lengths of time. The signal intensity, S, just after the 90° pulse is plotted against pulse interval τ between 180 and 90° pulse. For clarity each reading at a given decomposition time is shifted horizontally by 100 msec.

which contains an energy gradient term (fourth order spatial derivatives of composition) in addition to the usual Fickian term (second derivatives). On the basis of this equation Cahn predicted several characteristics associated with the early stages of spinodal decomposition which can be summarized as follows.

First, because of the gradient energy term, it tends to selectively promote the continuous but rapid growth of sinusoidal composition modulation of a certain wavelength, λ_m. One should therefore observe a separation behavior in which the composition of phases changes continuously with time while the spacing of the phase pattern remains nearly constant, at least in the early stages of decomposition.

Second, the diffusion coefficient must be negative (uphill diffusion).

Third, for isotropic materials the waves have random orientations and phase angles so that the spinodal structure should be almost uniform yet random and interconnected. Connectivity of phases is an important morphological feature of spinodal which should be observed when the volume fraction of one phase exceeds about 15%. However, it has been pointed out that the presence of such a morphological feature alone is not a proof that phase separation occurred by spinodal mechanism.[4,5,18] If on the other hand one can detect either of the first two characteristics in the phase separation, then the spinodal mechanism must have occurred.[4] In the above discussion we have not included the contribution of coherent strain energy because it is deemed insignificant in an amorphous polymer above the glass temperature.

The difference between this mechanism and nucleation and growth is therefore quite apparent. In nucleation and growth the new phase starts from nuclei which then proceed to grow in extent. The molecules that feed the new phases follow the ordinary transport phenomenon by downhill diffusion (positive coefficient of diffusion). The structure is clearly two phase and the composition of the precipitating phases is invariant at any time.

From the above description of the two decomposition mechanisms, it is clear that the pulsed nmr technique provides a powerful and convenient tool for detecting spinodal decomposition. As seen in Figure 11 and Table I where the pulsed nmr data are given for the 50:50 mixture annealed at 130° for various lengths of time, the volume fraction of the PS-rich phase as indicated by the long T_1 component remains nearly constant at 35% while the composition in each phase as indicated by the two T_1's changes continuously with the decomposition time. The results are therefore clear proof that the sample did undergo phase separation by spinodal mechanism. In addition, as will be shown

Table I
Spin-Lattice Relaxation Time, T_1 Analysis at 50° for PS-PVME = 50:50 Compatible Polymer Mixtures Decomposed at 130° for Various Lengths of Time

Decomposition time	T_1		Long T_1 component, %	PVME % in PS-rich phase
	Long T_1, msec	Short T_1, msec		
Original		195		
20 sec	390 ± 30	115 ± 15	40 ± 8	29.5 ± 1.5
40 sec	375 ± 20	130 ± 10	35 ± 6	30 ± 1
1 min	420 ± 20	120 ± 10	37 ± 6	28 ± 1
2 min	410 ± 10	115 ± 5	39 ± 4	27.5 ± 0.5
4 min	530 ± 10	112 ± 5	38 ± 4	23.5 ± 0.5
8 min	610 ± 15	120 ± 5	31 ± 4	21.5 ± 0.5
32 min	680 ± 15	115 ± 5	33 ± 4	19.5 ± 0.5

later, the coefficient of diffusion in the early stages of phase separation is negative. Thus it is not surprising that the sample morphology shows a high degree of interconnectivity of phases and uniformity of texture at early stages of decomposition, Figure 10b.

Since all samples treated under open circle conditions (Figure 7) exhibited similar morphological features as the 50:50 sample heat treated at 130° (see Figures 8, 10b, and 10c), it may be inferred that spinodal mechanism took place while the samples underwent these isothermal aging treatments. If one accepts this to be the case then the characteristic thermochromatic behavior displayed by sample PS-PVME = 20:80 during the thermal cycling, Figures 3, 4, and 6, would appear to be a significant manifestation of the spinodal mechanism. The precise reason for this unusual behavior cannot be given although it is apparently related to the formation and disappearance of the interconnected phase pattern (*cf.* Figure 10b).

If the phase separation under the open circle conditions is due to spinodal mechanism, it would be reasonable to ascribe the decomposition phenomenon under the filled circle conditions to nucleation and growth. This view is supported by the morphological observations, Figures 9 and 10a, and by the fact that the thermochromatic results, Figures 2 and 5, differ radically from those obtained under open circle conditions. Moreover, as may be seen in Figure 7, all the filled circles are located near the phase separation curve but away from ϕ_{min}. This region is likely to be within the metastable gap where decomposition by nucleation and growth is favored. It follows from these considerations that the so-called spinodal which separates the metastable region from the unstable region should fall somewhere between the regions dotted with open and filled circles. As expected this spinodal line approaches the phase separation curve near ϕ_{min}.

As in the case of spinodal decomposition, it should in principle be possible to detect nucleation and growth by pulsed nmr measurements. However, because of the proximity of filled circles with the phase separation curve (*cf.* Figure 7), there was some difficulty in detecting the change in the spin–lattice relaxation time of the minor phase. Nevertheless, this technique should be useful in systems which show a large metastable gap in its phase diagram.

We will now attempt to determine or estimate at least the orders of magnitudes of the parameters which describe the kinetics of initial stages of spinodal decomposition. According to the theory developed by Cahn[4] for the one dimensional problem, the composition change during the initial stages of phase separation can be described by

$$c - c_0 = \sum_{\text{all }\beta} A(\beta) e^{R(\beta)t} \cos \beta x \tag{2}$$

where c is the composition and c_0 the average composition before phase separation, β is the wave number of the sinusoidal composition modulation; t and x are respectively time and space variables, and $R(\beta)$ is given by

$$R(\beta) = -\tilde{D}\left[1 + \frac{2K}{f''}\beta^2\right]\beta^2 \tag{3}$$

Here $\tilde{D}$ is the coefficient of diffusion, K is the gradient-energy coefficient, and f'' is the second derivative of the Gibbs free energy with respect to composition c.

If the parameters in eq 3 are such that $R(\beta)$ is negative, then, from eq 2, the composition modulation will decay with time. On the other hand, positive $R(\beta)$ will result in rapid growth of the amplitude. $R(\beta)$ is therefore the major controlling factor of the spinodal mechanism. The value of β at which $R(\beta)$ becomes zero is defined as the critical wave number, β_c, and is given by

$$\beta_c = (-f''/2K)^{1/2} \tag{4}$$

In other words, initial composition fluctuations with wave numbers greater than β_c will decay while those with wave numbers less than β_c will grow during the spinodal instability.

In terms of β_c, eq 3 can be rewritten as

$$R(\beta) = -\tilde{D}\left[1 - \frac{\beta^2}{\beta_c^2}\right]\beta^2 \tag{5}$$

Since $R(\beta)$ has a sharp maximum at $\beta_m = \beta_c/2^{1/2}$, the initial composition fluctuation with this wave number β_m will have the maximum growth rate. Consequently the kinetics of the spinodal mechanism is dominated by the growth of this particular composition modulation and eq 2 can be approximated by the following expression

$$c - c_0 = A(\beta_m) e^{R(\beta_m)t} \cos \beta_m x \tag{6}$$

with

$$R(\beta_m) = -\tfrac{1}{2}\beta_m^2 \tilde{D} \tag{7}$$

We will first compute the coefficient of diffusion $\tilde{D}$ from eq 6 and 7 using the morphological and nmr data. For this purpose, the composition c will be identified with the concentration of PVME in the PS-rich phase. From eq 6 the total reduction Q of PVME in the PS-rich phase during the decomposition is approximately equal to

$$Q = \left[\left|\int_{\frac{\pi}{2\beta_m}}^{\frac{3\pi}{2\beta_m}} (c - c_0)\, dx\right|\right]^3 = \left[\frac{2}{\beta_m}A(\beta_m)\right]^3 e^{3R(\beta_m)t}$$

so that

$$\ln Q = 3 \ln\left[\frac{2}{\beta_m}A(\beta_m)\right] + 3R(\beta_m)t \tag{8}$$

Thus a plot of ln Q against t should yield a straight line with a slope equal to $3R(\beta_m)$. In Figure 12 the quantity ln Q obtained from nmr measurements (last column of Table I) is plotted against the decomposition time. Despite a slight scatter, the curve clearly shows a positive slope or a positive $R(\beta_m)$ which is evidence that spinodal reaction took place in the sample. The increasing trend of ln Q is approximately linear up to about 4 min beyond which it tends to level off sharply. If one draws a straight line through the points lying between 0 and 4 min, a slope of 1.15×10^{-3} sec^{-1} is obtained. This yields a $R(\beta_m)$ of

$$R(\beta_m) = 3.82 \times 10^{-4}\ sec^{-1} \tag{9}$$

The value of β_m can be estimated from the morphological

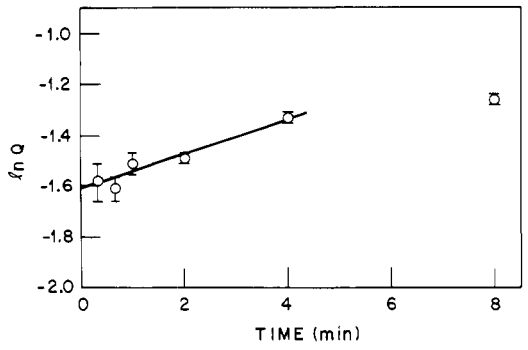

Figure 12. Logarithm of total change of PVME concentration in PS-rich phase *vs.* decomposition time. Data based on the results listed in the last column of Table I.

pattern shown in Figure 10b assuming that the average spacing (~0.6 μm) corresponds to the half-wavelength of the fastest growing wave β_m. Thus

$$\beta_m = 2\pi/\lambda_m = 5.24 \times 10^4 \text{ cm}^{-1} \quad (10)$$

Using the values of $R(\beta_m)$ and β_m in eq 9 and 10, the coefficient of diffusion $\tilde{D}$ is found to be

$$\tilde{D} = -\frac{2R(\beta_m)}{\beta_m^2} = -2.8 \times 10^{-13} \text{ cm}^2/\text{sec} \quad (11)$$

Although the above value of $\tilde{D}$ may only be approximate, the negativeness of $\tilde{D}$ is beyond question. This is again a positive proof of spinodal decomposition in the 50:50 mixture at 130°.

To compute the value of K which appears in eq 3 and hence in eq 2, we resort to a relation obtained by van Aartsen[6]

$$K/B = l^2/6 \quad (12)$$

where l is the Debye range of molecular interaction[15] and B is a constant which enters an expression for the interaction parameter χ *via* eq 13. Here A is another constant, RT has

$$\chi = A - (BV_1/RT) \quad (13)$$

the usual meaning, and V_1 is the molar volume of polymer mer 1 which is identified with PVME. It is therefore necessary to estimate both l and B before K can be computed.

In the previous study on the compatibility of the PS–PVME = 55:45 mixture,[2a] χ is −0.69 at 30° and −0.6 at 50°. If χ for the 50:50 mixture is assumed to have the same values at these two temperatures, then the two unknowns A and B can be found from the simultaneous equations obtained by substituting the two sets of numbers into eq 13.

$$A = 0.76 \quad (14)$$

$$B = 15.8 \text{ cal/(cm}^3 \text{ of PVME)} \quad (15)$$

It is reasonable to believe that A and B do not remain invariant with temperature. In fact, if both are temperature independent, the parameter χ at the phase separation temperature (~100°) would be −0.42, a value apparently too low. It is generally accepted that as the lower critical solution temperature is approached from the low-temperature side, the major cause of incompatibility is the decreasing contribution of the entropy of mixing. It is likely that A changes more rapidly than B near the cloud point. Therefore, we assume that B retains the same value 15.8 cal/cm^3 at the phase separation temperature; the corresponding value of A is 1.18 so that χ approaches zero at that temperature. If we assume A is constant, then B is 10.2 cal/(cm^3 of PVME). In any case, the order of B is not affected so much and only experiments can give the necessary data, which may be very difficult at this temperature range.

The range of molecular interaction l can be evaluated from a variant of another relation derived by van Aartsen[6]

$$\lambda_m = 2\pi l \left[3\left(\frac{T}{T_s} - 1\right)\right]^{-1/2} \quad (16)$$

where T_s is the spinodal temperature.

The expression differs from the one given by van Aartsen[6] in the term $((T/T_s) - 1)$ because the miscibility gap here is associated with a lower critical solution temperature. Now from the morphological patterns shown in Figures 10b and 10c, the wavelength λ_m of the dominant composition modulation is found to be about 1.2 μm at 130° and 0.9 μm at 140°.

By substituting these two sets of numbers separately into eq 16 and solving the resultant simultaneous equations for l and T_s one finds

$$\begin{aligned} l &= 580 \text{ Å} \\ T_s &= 391°\text{K} \quad (118°) \end{aligned} \quad (17)$$

Although the computed T_s is slightly lower than 120° at which temperature the 50:50 mixture was found to phase separate by nucleation and growth, this is not surprising since as T_s is approached from the unstable region the spinodal mechanism will slow down and vanish whereas the rate of nucleation and growth does not become zero there. Consequently one finds nucleation and growth rather than spinodal mechanism at T_s.

The magnitude of l can be checked independently by noting that it should be in the order of root-mean-square radius of gyration,[19] $\langle s^2 \rangle^{1/2}$

$$\langle s^2 \rangle^{1/2} = \frac{\alpha}{\sqrt{6}} \left(\frac{C_\infty b^2}{M_0}\right)^{1/2} M^{1/2} \quad (18)$$

where α, C_∞, b, M_0, and M are respectively the expansion factor, characteristic ratio, bond length, average molecular weight per backbone bond, and polymer molecular weight.[20] For PS, $C_\infty = 10$, $b = 1.53$ Å, $M_0 = 29$, and $M = 2 \times 10^5$ so that from eq 18, $\langle s^2 \rangle^{1/2} = 125\alpha$ Å. There are no data for α of the PS–PVME compatible mixture. But α should be in the range of 1.5–2.0.[21] The magnitudes of $\langle s^2 \rangle^{1/2}$ and l are therefore comparable.

Consequently with the help of eq 12, 15, and 17, K is found to be

$$\begin{aligned} K &= 8.9 \times 10^{-11} \text{ (cal cm}^2\text{)/(cm}^3 \text{ of PVME)} \\ &= 3.7 \times 10^{-3} \text{ (erg cm}^2\text{)/(cm}^3 \text{ of PVME)} \end{aligned} \quad (19)$$

Once K is known, f'' can be estimated from eq 4 by noting that $\beta_c = 2^{1/2}\beta_m$, thus

$$\begin{aligned} f'' &= -4K\beta_m^2 \\ &= -0.97 \text{ cal/(cm}^3 \text{ of PVME)} \\ &= -4.1 \times 10^7 \text{ erg/(cm}^3 \text{ of PVME)} \end{aligned} \quad (20)$$

We have now obtained an estimate of all parameters which describe the kinetics of spinodal decomposition. To our knowledge, our effort in computing all the kinetic parameters in spinodal decomposition represents the first attempt of its kind in the study of polymer mixtures. Whether these values have the right magnitude cannot be ascertained at this time but on the basis of experimental results (*cf.* Table I) they appear to have at least the correct sign. In this connection, it is of interest to note that typical orders of magnitude of these parameters in metallic systems are[5] $\tilde{D} \sim -10^{-18}$ cm^2/sec, $K \sim 10^{-5}$ erg/cm (atomic fraction)$^{-2}$, and $f'' \sim -10^{-10}$ erg/cm^3 (atomic fraction)$^{-2}$.

Conclusion

The PS–PVME system is found to phase separate by spinodal mechanism or by nucleation and growth depending on composition and temperature. The spinodal decomposition is confirmed by pulsed nmr data of a 50:50 mixture isothermally annealed at 130°, which shows a continuous change in composition of new phases while the volume of the new phases remains constant during phase separation. Further evidence of spinodal mechanism is found in the negativeness of the diffusion coefficient and in the interconnected morphological pattern of the sample.

Large differences in light transmission and morphological behavior are noted during the early stages of decomposition under the two mechanisms. Samples which decompose by nucleation and growth during a heating cycle show a normal hysteresis in their thermochromatic properties with no residual turbidity, whereas samples decomposed by spinodal reaction exhibit unusual thermochromatic behavior with some turbidity remaining at the end of the heating cycle. The residual turbidity depends upon composition and reaches its maximum at the PS concentration of 0.2. Reasons for this anomalous behavior are not clear but it is probably related to the formation and disappearance of the interconnected phase pattern. Further study on this subject may be warranted.

The morphological features for the two mechanisms are different not only in their overall patterns but also in the rate with which these patterns are developed. In the spinodal decomposition, the formation of the interconnected pattern is rapid and the texture is uniform and becomes finer with an increase of the annealing temperature. In nucleation and growth, on the other hand, the domains of precipitating phases are discrete and their formation is relatively slow.

Finally the basic parameters governing the kinetics of spinodal decomposition are estimated using the nmr data obtained for a 50:50 mixture heat treated at 130°. The results together with other thermodynamic constants for the mixture are summarized below.

$$\tilde{D} \approx -2.8 \times 10^{-13}\ \text{cm}^2/\text{sec}$$

$$K \approx 3.7 \times 10^{-3}\ (\text{erg cm}^2)/(\text{cm}^3\ \text{of PVME})$$

$$f'' \approx -4.1 \times 10^{7}\ \text{erg}/(\text{cm}^3\ \text{of PVME})$$

$$T_s \approx 118°$$

$$l \approx 580\ \text{Å}$$

$$A \approx 1.18$$

$$B \approx 15.8\ \text{cal}/(\text{cm}^3\ \text{of PVME})$$

Acknowledgment. We are grateful to Dr. D. C. Douglass for making available to us his pulsed nmr instrument. We are also grateful to him and Drs. E. Helfand and R.-J. Roe for valuable discussions.

References and Notes

(1) Resident visitor: Tokyo Research Laboratory, Bridgestone Tire Co., Ltd., Tokyo, Japan.
(2) (a) T. K. Kwei, T. Nishi, and R. F. Roberts, *Macromolecules*, **7**, 667 (1974); (b) T. Nishi and T. K. Kwei, *Polymer*, in press.
(3) L. P. McMaster, *Macromolecules*, **6**, 760 (1973).
(4) J. W. Cahn, *J. Chem. Phys.*, **42**, 93 (1965); *Trans. AIME*, **242**, 166 (1968).
(5) J. E. Hilliard, "Phase Transformations," American Society for Metals, 1970, Chapter 12.
(6) J. J. van Aartsen, *Eur. Polym. J.*, **6**, 919 (1970).
(7) C. A. Smolders, J. J. van Aartsen, and A. Steenbergen, *Kolloid-Z. Z. Polym.*, **243**, 14 (1971).
(8) L. P. McMaster, *Amer. Chem. Soc., Div. Polym. Prepr.*, **15**, 254 (1974).
(9) G. P. Jones, D. C. Douglass, and D. W. McCall, *Rev. Sci. Instrum.*, **36**, 1460 (1965).
(10) J. E. Anderson and W. P. Slichter, *J. Phys. Chem.*, **69**, 3099 (1965).
(11) D. C. Douglass and G. P. Jones, *J. Chem. Phys.*, **45**, 956 (1966).
(12) D. C. Douglass and V. J. McBrierty, *J. Chem. Phys.*, **54**, 4085 (1971).
(13) M. Bank, J. Leffingwell, and C. Thies, *J. Polym. Sci., Part A-2*, **10**, 1097 (1972).
(14) N. J. Trappeniers, C. J. Gerritsma, and P. H. Oosting, *Physica (Utrecht)*, **30**, 997 (1964).
(15) V. J. McBrierty, *Polymer*, **15**, 509 (1974).
(16) R. Koningsveld and A. J. Staverman, *J. Polym. Sci., Part A-2*, **6**, 349 (1968).
(17) K. Šolc, *Macromolecules*, **3**, 665 (1970).
(18) T. P. Seward III, D. R. Uhlmann, and D. Turnbull, *J. Amer. Ceram. Soc.*, **51**, 634 (1968).
(19) P. Debye, *J. Chem. Phys.*, **31**, 680 (1959).
(20) P. J. Flory, "Statistical Mechanics of Chain Molecules," Wiley, New York, N.Y., 1969.
(21) P. J. Flory, "Principles of Polymer Chemistry," Cornell University Press, Ithaca, N.Y., 1953.